

A high-throughput proteomics screen identifies novel substrates of
Death Associated Protein Kinase

Shani Bialik, Hanna Berissi, and Adi Kimchi

Dept. of Molecular Genetics, Weizmann Institute of Science, Rehovot, Israel 76100

Corresponding author: Adi Kimchi
Phone: 972-8-934-2428
Fax: 972-8-931-5938
email: adi.kimchi@weizmann.ac.il

Running Title: Proteomics screen for DAP-kinase substrates



Abbreviations

CaM, calmodulin

CaMKK, Ca²⁺/CaM-dependent Protein Kinase Kinase

DAPk, Death Associated Protein Kinase

IFN γ , interferon- γ

MLC, myosin II regulatory light chain

TGF- β , Transforming growth factor β

ZIPk, ZIP-kinase

Summary

Death Associated Protein Kinase (DAPk) is a Ser/Thr kinase whose activity is necessary for different cell death phenotypes. While its contribution to cell death is well established, only a handful of direct substrates have been identified, which do not fully account for DAPk's multiple cellular effects. In order to identify such substrates on a large scale, we developed an *in vitro*, unbiased, proteomics-based assay to search for novel DAPk substrates. Biochemical fractionation and mass spectrometric analysis was used to purify and identify several potential substrates from HeLa cell lysate. Here we report the identification of two such candidate substrates, the ribosomal protein L5 and Mcm3, a replication licensing factor. While L5 proved to be a weak substrate, Mcm3 was efficiently and specifically phosphorylated by DAPk on a unique site, Ser160. Significantly, DAPk phosphorylates this site *in vivo* upon over-expression in 293T cells. Activation of endogenous DAPk by increasing intracellular Ca^{2+} also leads to increased phosphorylation of Mcm3. Importantly, shRNA-mediated knock-down of endogenous DAPk blocks both basal phosphorylation and Ca^{2+} -induced phosphorylation, indicating that DAPk is both necessary and sufficient for Mcm3 Ser160 phosphorylation *in vivo*. Identification of Mcm3 as an *in vivo* DAPk substrate indicates the usefulness of this approach for identification of physiologically relevant substrates that may shed light on novel functions of the kinase.

Introduction

DAP-kinase (DAPk), a Ca^{2+} /calmodulin (CaM) activated Ser/Thr kinase which localizes to the cytoskeleton, has been linked to cell death and is a potent tumor suppressor (reviewed in 1). Originally identified in a screen for genes whose functions were necessary for IFN- α -induced death (2), it has since been shown to be necessary for the regulation or execution of cell death in response to numerous stimuli, including death receptor activation (3), TGF- β (4), oncogene expression (5), UNC5H2 signaling (6), ceramide (7-8), and matrix detachment (9). The specific cellular phenotype induced by DAPk activity can vary from one cell setting to another. It has been linked to both type I apoptotic and type II autophagic cell deaths, in both caspase-dependent and caspase-independent manners (1). Specifically, DAPk expression can lead to various actin-dependent death-associated morphologic changes, which include membrane blebbing and cell rounding (e.g. 10-11). Detachment from the extra-cellular matrix often accompanies these phenotypes, due to inhibition of integrin function (12). Even in the absence of cell death, DAPk's effects on the cytoskeleton can lead to the induction of stress fiber formation (13) and interference with cell polarity and directed cell motility (14). DAPk has also been linked to p53-dependent apoptosis through the induction of p53 in a p19ARF-dependent manner (5), and can lead to the upregulation of autophagy (11). In addition to the chromatin fragmentation that accompanies caspase-dependent apoptosis (e.g. 4-6), DAPk expression can also lead to caspase-independent nuclear changes that include chromatin condensation (11). Each of these phenotypes can be considered an independent functional arm of DAPk.

Catalytic activity is required for all DAPk-associated phenotypes, implying that phosphorylation of specific substrates mediates the various functional arms. To date, only a limited number of substrates have been identified. These include the regulatory light chain of

myosin II (MLC), whose phosphorylation and subsequent activation of myosin-based contractility leads to membrane blebbing (10,13,15-16). A second substrate identified is syntaxin-1A, a component of the v-SNARE complex, which mediates docking and fusion of synaptic vesicles with the membrane (17). While kinetically, syntaxin-1A is an efficient *in vitro* DAPk substrate, its physiologic relevance is not yet known. DAPk was also shown to phosphorylate ribosomal protein S6, thereby reducing translation rates in reticulocyte lysates (18). DAPk may also participate in kinase signaling cascades, as it has been shown to phosphorylate and regulate other kinases. For example, phosphorylation of the highly related ZIP-kinase (ZIPk) influences its intracellular localization and enhances its death-promoting activity (19). DAPk can also efficiently phosphorylate Ca²⁺/CaM-dependent Protein Kinase Kinase (CaMKK), *in vitro* and *in vivo*, which inhibits the latter's ability to undergo CaM-activated autophosphorylation *in vitro* (20). During oxidative stress, DAPk phosphorylates Protein Kinase D, leading to activation of JNK and subsequently, caspase-independent cell death (21). While identification of these substrates has shed light some of DAPk's mechanisms of action, there are still many gaps that remain in our understanding of how DAPk activity leads to the multiple functional outcomes discussed above. In order to fully fill in these gaps, a more thorough understanding of DAPk's complete substrate profile needs to be attained.

Here we undertook a large-scale, unbiased proteomics based screen whose aim was to identify DAPk substrates *in vitro*, to be followed by *in vivo* confirmation. This was based on a recently described method for searching for kinase substrates, called KESTREL, which has been successfully used to identify substrates for several closely related kinases (22,23). In this manner, we identified two novel DAPk substrates, ribosomal protein L5 and the Mcm3 replication initiation factor.

Experimental Procedures

Plasmids and Reagents

Plasmids encoding N-terminal FLAG and HA-tagged human full length DAPk, (pcDNA3-DAPk), the activated kinase deleted of its calmodulin regulatory domain (pcDNA3-DAPk Δ CaM), or the catalytically inactive mutant (pcDNA3-DAPkK42A) have been described previously (10). A pASK-IBA3 vector encoding the catalytic domain of DAPk (aa 1-285) tagged at its C-terminus with streptavidin was obtained from M. Watterson (Northwestern University, Chicago, IL) and used to produce recombinant DK1. pcDNA3 encoding the non-relevant protein luciferase (Luc) was used as a control. Flag-tagged L5 was generated by PCR cloning of the rat L5 cDNA (kind gift of O. Meyuhas, Hebrew University, Jerusalem, Israel) into pcDNA3. Flag-tagged human Mcm3 in pcDNA3 was a kind gift from Dr. M. Gossen, Max-Delbruck-Center for Molecular Medicine, Berlin, Germany (25). Ser160 was mutated to either Ala or Asp by PCR-based site directed mutagenesis using the QuickChange Mutagenesis kit (Stratagene) according to the recommended protocol. pSuper-based vectors containing shRNA targeting DAPk (nucleotides 5776-5794, accession number NM_004938.2) or Hc-Red (nucleotides 99-117, accession number AF363776) were used for knock-down experiments. Chemicals and inhibitors were purchase from Sigma-Adrich (Rehovot, Israel), unless otherwise indicated.

Cell Culture

293T human embryonic kidney cells and HeLa cells were grown in DMEM (Biological Industries, Beit Haemek, Israel) supplemented with 10% fetal bovine serum, L-glutamine (2 mM), penicillin (50 U/ml) and streptomycin (50 μ g/ml, Gibco BRL). Cells were transiently transfected by the Ca²⁺-phosphate precipitation method. When indicated, cells were treated with

5 μ M ionomycin for 30 min. For experiments using shRNA, cells were transfected with pSuper-based vectors encoding DAPk shRNA or control Hc-Red shRNA for 5 days before treatment with ionomycin.

Substrate identification

For large scale purification, HeLa cells were grown until confluency, collected, lysed in lysis buffer (50 mM Tris, pH 7.6, 150 mM NaCl, 2 mM EDTA, 1% NP-40, in the presence of 1% protease inhibitor cocktail and 1 mM PMSF) and sonicated. Following dialysis against 25 mM Tris, pH 7.4, NH_4SO_4 was added to the lysate to achieve a final concentration of 25% salt. Proteins were allowed to precipitate on ice, and the pellet was collected by centrifugation. The resulting supernatant was then subjected to further salt precipitation, repeatedly, to obtain 40, 50, 60 and 80% NH_4SO_4 precipitants. All pellets were resuspended in 25 mM Tris, pH 7.4 and further dialyzed against 25 mM Tris, pH 7.4. 1% of the dialyzed protein was subjected to an *in vitro* kinase assay with recombinant catalytic domain of DAPk (DK1) to monitor the presence of particular substrates. The remaining portion of each salt precipitant was applied to a HiTrap Phenyl-HP hydrophobic column (Pharmacia) after addition of NH_4SO_4 to a final concentration of 1M. The column was washed with buffer, and then proteins eluted over a NH_4SO_4 concentration gradient ranging from 1-0M. Fractions collected were dialyzed against 25 mM Tris, pH 7.4, and concentrated on a YM-10 CentriPlus Spin column (Millipore) to approximately 1/10 volume. A small portion (1-5%) of the total protein from selected fractions was assayed with DK1 for the presence of substrate. Fractions selected for the highest substrate content were resolved by SDS-PAGE in parallel with the products of the *in vitro* kinase assay. The half of the gel containing the kinase assay was silver stained, to detect the lower levels of protein present, while the remaining half of the gel was stained with Gelcode (Pierce). The location of each substrate on

the gel was denoted by comparison of the autoradiogram and silver stained gels, and the equivalent portion of the gel was then excised from the Gelcode-stained gel. The protein sampled was digested with trypsin, fractionated into individual peptides by liquid chromatography, and then analyzed by mass spectrometry (MS/MS) at the Biological Mass Spectrometry unit of the Weizmann Institute of Science using an API Q-Star Pulsarⁱ Electrospray-Quadrupole TOF tandem mass spectrometer with a collision cell (MDS-Sciex, Canada, ABI) equipped with a nanoelectrospray source (MDS Proteomics, Odense, Denmark). Peak lists were generated from the raw data using Analyst QS1.1 and BioAnalyst 1.1.5 (MDS Sciex) and Mascot 2.1 (Matrix Science) software. Centroid and de-isotoping parameters were used, and peaks less than 10% of the maximum were removed from analysis. A Mascot MS/MS ions search of the Swiss-Prot 51.0 human database (27,0778 entries, 99412397 residues) was performed, with a peptide tolerance of ± 0.8 Da and a MS/MS tolerance of ± 0.8 Da. Up to two missed cleavages, 4 positive charges, and modifications by oxidation, deamidation and carbamidomethylation were allowed.

Protein Purification and Immunoprecipitation

DK1 was expressed in TOP10 bacteria (Invitrogen) upon induction with tetracycline, and affinity purified from bacterial lysates using the StrepTactin column (Genosys Biotechnologies) according to the manufacturer's instructions. Full length Flag-DAPk or Flag-tagged substrates were expressed in 293T cells, which were lysed in B buffer (20 mM HEPES, pH 7.6, 100 mM KCl, 0.5 mM EDTA, 0.4%NP-40, 20% glycerol), supplemented with protease inhibitors. For experiments using DAPk K42A, which expresses much lower levels than the WT kinase, cells expressing either K42A or WT DAPk constructs were first treated with the actin depolymerizing agent latrunculin B (20 μ M) for 30 min to release all of the kinase from the actin cytoskeleton

and then immediately lysed in B Buffer. Extracts were immunoprecipitated with an anti-Flag M2 monoclonal antibody conjugated to protein G beads and proteins were eluted with excess Flag peptide. Mcm3-bound beads were first washed stringently in 0.5 M KCl and 0.5 M LiCl₂ to remove co-precipitating kinases that resulted in high basal levels of phosphorylation. For immunoprecipitation of phosphorylated Mcm3, cells were lysed in PLB (10 mM NaPO₄ pH 7.5, 5 mM EDTA, 100 mM NaCl, 1% Triton, 0.5% Na deoxycholate, 0.1% SDS) containing protease and phosphatase inhibitors (100 nM okadaic acid, 20 mM β -glycerophosphate, 1 mM NaF), and immunoprecipitated with monoclonal anti-Mcm3 antibodies (Stressgen) pre-bound to protein G agarose.

Kinase assays

Kinase assays of total cell lysate or fractionated lysates followed a modified protocol based on the KESTREL method described in (22). In brief, samples were incubated with DK1 (0.5 mg) in DK kinase buffer (50 mM β -glycerophosphate, 20 mM MnCl₂) in the presence of 57 nM (5 μ Ci) [γ -³³P]ATP (Amersham) and the following inhibitors: 1 mM PMSF, 1% protease inhibitor cocktail, 1 mM NaF, 5 mM EGTA, 10 μ M PKI, for 2 min at 30°C. Reactions were terminated by the addition of sample buffer and boiled prior to electrophoresis on SDS-polyacrylamide gels. Depending on the amount of protein present, gels were either silver stained or stained with Gelcode, dried and exposed to MR X-ray film (Kodak). For kinase assays using purified Flag-tagged substrate, reactions were incubated for 10 min with DK1 as described above. For assays using full length DAPk as the kinase, immunopurified Flag-DAPk and Flag-tagged substrate at kinase:substrate molar ratios of ~1:5 or 1:10 were incubated for 10 minutes at 30°C in kinase buffer (50mM Hepes pH 7.5, 20mM MgCl₂) supplemented with 0.16 μ Ci/ μ l [γ -³³P]ATP, 50 μ M ATP, 1 μ M bovine calmodulin, and 0.5 mM CaCl₂. For stoichiometric

analysis, kinase assays were performed over a time-course ranging from 1 min to 2 h. Reactions were terminated by boiling in SDS-loading buffer, and were resolved on 7.5% acrylamide gels, which were stained with Gelcode and dried. Levels of ATP incorporated were measured by phosphoimaging and comparison to a standard curve of known ATP concentrations. For determination of K_m and V_{max} values, a peptide derived from the Mcm3 phosphorylation site was synthesized and used in P-81 Whatman filter assays. 20 ng DK1 was incubated for 15 min at 30°C with increasing concentrations of peptide (0.25-1000 μ M) in reaction buffer of 50 mM Hepes, pH 7.5, 20 mM $MgCl_2$, 100 μ M ATP and 4 μ Ci [γ - ^{33}P]ATP. Reactions were applied to P-81 filters and washed extensively in 1% phosphoric acid. Total counts were measured by scintillation counting. Total levels of ATP incorporated were calculated and plotted against substrate concentration. Double-reciprocal plots were generated and analyzed by linear regression to obtain kinetic parameters.

Western Blot Analysis

Total cell lysates, protein immunoprecipitates or kinase assays were resolved on 7.5% or 10% polyacrylamide gels, transferred to nitrocellulose membranes blots and reacted with monoclonal antibodies to Mcm3 (Stressgen), DAPk (clone #55, Sigma), actin (Sigma) or ZIPk (BD Transduction Laboratories), or affinity purified rabbit polyclonal antibodies to the Mcm3 phosphopeptide KKTIERRYpS¹⁶⁰DLT (generated by PhosphoSolutions, Aurora, Co). Secondary antibodies consisted of HRP-conjugated goat anti-mouse or anti-rabbit antibodies (Jackson ImmunoResearch), which were detected by SuperSignal enhanced chemiluminescence (Pierce).

Results

In vitro screen for DAPk substrates

In order to identify novel substrates of DAPk whose phosphorylation may mediate the kinase's various functional cellular effects, an unbiased, high throughput screen was undertaken. An *in vitro* kinase assay was performed on HeLa cell lysate in the presence of a recombinant protein that consisted of the catalytic domain of DAPk (DK1). DK1 lacks the regulatory domains of DAPk, and is constitutively active even in the absence of Ca^{2+} /CaM. Furthermore, it lacks the major autophosphorylation sites of the full length kinase (24). To suppress the activity of endogenous kinases present in the lysates, specific kinase inhibitors were added to the reaction buffer (i.e. PKI to inhibit PKA, and EGTA to inhibit Ca^{2+} -dependent kinases). Furthermore, the reactions were run under stringent conditions including short incubation times and the use of limiting quantities of Mn^{2+} -ATP ($[\text{P}^{33}]$). Preliminary experiments confirmed that the replacement of the usual Mg^{2+} with Mn^{2+} in the reaction buffer had no effect on DK1 activity (data not shown). The addition of DK1 to the reaction mix led to the phosphorylation of up to 9 prominent substrates, which were referred to as S1-S9 (Fig. 1). The strongest phosphorylation was observed at a band of 20 kDa (S2), which corresponds to the molecular weight of MLC, a known *in vitro* and *in vivo* substrate of DAPk (13,15-16). In fact, a protein at the same position as S2 was recognized by antibodies to MLC, suggesting that S2 is MLC (data not shown). The identification in this manner of a known DAPk substrate validates this strategy as an effective tool for identifying relevant substrates.

In order to semi-purify substrates to enable identification, HeLa cell lysate was subjected to consecutive fractionation steps. The first round consisted of stepwise precipitation with

NH_4SO_4 (i.e., 25%, 40%, 50%, 60% and 80% final concentration). The majority of proteins precipitated at the 50% and 60% NH_4SO_4 concentrations. Each salt fraction was then applied to a phenyl-HP hydrophobic column and proteins were eluted with decreasing concentrations of NH_4SO_4 . DK1 kinase assays were performed on 1-5% of the total protein in selected fractions. Resolution of the kinase reactions by electrophoresis, followed by silver staining of the gel and autoradiography, revealed the elution profiles of individual substrates. For example, the strongest S5 signal was observed to elute in fractions 19-22 upon fractionation of the 60% salt cut (Fig. 2A). Interestingly, S5 was a weak and barely detectable substrate in the original total cell lysate, yet gave rise to a strongly phosphorylated band after the final fractionation. This enhanced reactivity may be due to enrichment of the total amount of protein present, or its isolation from additional cellular factors that inhibit its phosphorylation. The S9 substrate, which was most prominent in the 50% NH_4SO_4 fraction, eluted in fractions 32-46 upon application to the column, with particular enrichment in fractions 36-42, corresponding to 0 mM salt (Fig. 2B).

In order to identify the proteins corresponding to individual substrates, specific fractions were subjected to more precise resolution on SDS-PAGE. For example, for S5 identification, fraction #20 from the corresponding column was resolved on a 12% gel. For S9 identification, fractions #36 and 41, from either end of the range of elution, were each resolved on 6% gels. In each case, the band that ran at the position of the substrate was excised from each lane and analyzed by mass spectrometry. The complete results for S5 and S9 are presented in Tables I and II. In each case, several candidate proteins were present in the band of interest, migrating at the position of the DAPk substrate. The abundance of a particular protein in the sample (i.e. a high score in the MS results) does not of necessity correlate with its likelihood to be the true

substrate; a strong phosphorylation signal may indicate a highly efficient substrate rather than high levels of protein present in the fraction. Thus, among the candidate proteins identified by MS, each was tested by *in vitro* kinase assays, until the true substrate was identified by the process of elimination. To this end, each candidate was expressed as a Flag-tagged protein in 293T, immunopurified with anti-Flag antibodies, and incubated with DK1 in *in vitro* kinase assays. Among the candidates for S5, annexin-II, failed to undergo phosphorylation (data not shown). In contrast, ribosomal protein L5 was phosphorylated in a specific manner by DK1 (Fig. 3A). Furthermore, full length DAPk phosphorylated the L5 protein in the presence of $\text{Ca}^{2+}/\text{CaM}$ (Fig. 3B). However, compared to the known DAPk substrate, MLC, L5 was a relatively weak substrate in these assays.

The S9 substrate, a 110 kDa protein, was of particular interest, since, like DAPk, it was insoluble in mild detergent buffers (data not shown). One of the highest scoring candidates for S9 identified by mass spectrometry was Mcm3, a component of the replication licensing complex which undergoes caspase-mediated cleavage during apoptosis (25,26). Addition of DK1 to Flag-tagged Mcm3 led to significant phosphorylation, comparable to the phosphorylation levels attained with equimolar concentrations of recombinant MLC (Fig. 4A). Mcm3 was also phosphorylated by full length DAPk in a $\text{Ca}^{2+}/\text{CaM}$ dependent manner, in contrast to α -actinin4, a second high scoring candidate for S9, which failed to undergo phosphorylation and is used here as a negative control (Fig. 4B). To exclude the possibility that the phosphorylation observed was due to a contaminating kinase that co-precipitated with DAPk, kinase assays were also performed with immunopurified DAPk K42A, a mutant which has greatly reduced catalytic activity. In contrast to the WT DAPk, K42A failed to induce phosphorylation of Mcm3, in the

absence or presence of $\text{Ca}^{2+}/\text{CaM}$ (Fig. 4C). Thus, the identity of the S9 substrate is confirmed as Mcm3.

Kinetic analysis of Mcm3 phosphorylation and mapping of the phosphorylation site

Analysis of the kinetics of phosphorylation of Mcm3 by full length DAPk indicated a time-dependent increase in phosphorylation, achieving a maximum of 0.7 mol of ATP incorporated per mol of Mcm3 after 1.5h (Fig. 4D). Longer incubations did not result in increased phosphorylation, as the overall activity of the kinase (including autophosphorylation) tended to decline beyond 2h. This suggests that there is one unique DAPk phosphorylation site within Mcm3.

A scan of the Mcm3 sequence indicated a potential DAPk phosphorylation site at Ser160, which matched a proposed consensus sequence for efficient phosphorylation (27) (Fig. 5A). A mutant Mcm3 in which Ser160 was changed to Ala was generated and subjected to *in vitro* kinase assays with full length DAPk. Significantly, mutation of Ser160 almost completely abolished the DAPk-dependent phosphorylation, without affecting the basal phosphorylation observed in the absence of DAPk (Fig. 5B). The difference in the degree of phosphorylation in the WT versus mutant Mcm3 constructs was more apparent upon comparison of reaction rates between increasing concentrations of either protein (Fig. 5C). To further confirm Ser160 as the site of modification by DAPk, an antibody was generated that specifically recognizes the phosphorylated Ser160 site. Increasing concentrations of both WT and Ser160A Mcm3 were subjected to *in vitro* kinase assays with DAPk, which were then western blotted with the phospho-specific antibody. The antibody recognized the wild type, but not mutant Mcm3, in a concentration dependent manner (Fig. 5D). Furthermore, a peptide derived from the region

encompassing the phosphorylation site, corresponding to the sequence KKTIERYS³⁰⁸DLT, was phosphorylated *in vitro* by DK1. To measure the efficiency of Mcm3 as a DAPk substrate, the rate of ATP incorporation was measured over increasing concentrations of peptide (Fig. 6A). Double-reciprocal plot analysis of the resulting curve predicted a K_m of 16 μ M and a V_{max} of 9.7 pmol ATP/min/pmol DK1 (Fig. 6B). These values are comparable to those reported for additional DAPk substrates, syntaxin1A, ribosomal protein S6 and CaMKK (18, 20). Thus DAPk phosphorylates Mcm3 on Ser160 in an efficient manner.

DAPk phosphorylates Mcm3 *in vivo*

The kinetic properties of Mcm3 are well in the range of physiologic substrate/kinase relationships. To verify that Mcm3 is in fact phosphorylated *in vivo* by DAPk, an activated form of DAPk lacking the Ca²⁺/CaM binding domain (Δ CaM), was introduced into 293T cells. As controls, the catalytically inactive K42A mutant and an irrelevant protein (Luc) were used. Total Mcm3 protein was immunoprecipitated from lysates from these transfected cells, which was then blotted with the phospho-specific antibody. Interestingly, Mcm3 exhibited a low degree of phosphorylation in control cells, which was significantly enhanced in cells expressing active DAPk (Fig. 7A). This phosphorylation required DAPk catalytic activity, as the levels were not enhanced by the presence of DAPk K42A.

In order to determine whether DAPk phosphorylates endogenous Mcm3 under conditions when it is not grossly over-expressed, endogenous DAPk was activated by inducing a rise in cellular Ca²⁺ by treating 293T cells with ionomycin for 30 min. Significantly, phospho-specific western blotting of Mcm3 immunoprecipitates from ionomycin treated cells indicated an enhanced phosphorylation of Mcm3 at the DAPk recognition site compared to control, non-

treated cells (Fig. 7B). To prove that the enhanced phosphorylation of Mcm3 on Ser160 was dependent on DAPk, and not due to other signaling effects of increasing cellular Ca^{2+} , shRNA was used to knock-down DAPk expression in cells treated with either DMSO or ionomycin. DAPk expression was successfully reduced following transfection with shRNA vectors targeted to DAPk, but not the Hc-Red control protein (Fig. 7C). Significantly, the ionomycin-induced phosphorylation of Mcm3 was partially abrogated by knock-down of DAPk. Thus DAPk is necessary for phosphorylation of Mcm3 at Ser160 in response to increases in cellular Ca^{2+} . The residual phosphorylation observed may be attributed to the low levels of DAPk still present, or to the activation of other Ca^{2+} -dependent kinases, such as DAPk's closely related homologue, DRP-1. In addition, phosphorylation of Mcm3 in the basal state was also partially dependent on DAPk. Again, the residual phosphorylation observed may be due to redundancy or to incomplete knock-down of DAPk. Nevertheless, these experiments prove that endogenous DAPk is responsible for phosphorylation of Mcm3 on Ser 160, both in the basal state and upon increases in cellular Ca^{2+} .

Discussion

Protein kinases are the most common mediators of signaling transduction, yet for many, the full repertoire of substrates which mediate their cellular effects is not known. It is no trivial task to identify physiologically relevant kinase substrates. For some kinases for which a consensus phosphorylation site has been determined, substrates can be predicted based on the presence of such sites within their published sequences. Phosphorylation must then be confirmed by *in vitro* and *in vivo* kinase assays. Unfortunately, for DAPk, there are not yet enough known substrates with similar phosphorylation sequences to reliably predict a phosphorylation consensus. In order to solve this problem, Watterson and co-workers used a positional scanning peptide library to generate an optimal peptide substrate sequence starting from the MLC phosphorylation sequence (27). The sequence obtained can theoretically be used to scan protein databases for substrates, and in fact was used to correctly predict the phosphorylation site within CaMKK (20) and more recently, ribosomal protein S6 (18). Database searches predict nearly 200 human proteins containing the proposed consensus. Several of these, however, have been subjected to experimental validation assays and proven not to be phosphorylated by DAPk (data not shown). Considering the large number of potential substrates, without additional data indicating the relevance of a particular candidate, it is technically impractical to experimentally assess each one. Moreover, the phosphorylation sites in other known DAPk substrates, such as syntaxin-1A (17) and the extra-catalytic domain of ZIPk (19), lack the critical features of the proposed consensus. Therefore, this phosphorylation sequence alone is not a definitive tool for predicting DAPk substrates. Other methods for identifying kinase substrates include screening peptide expression libraries, which are limited since the targets are not in their native form and are not full length proteins. Several years ago,

an alternative approach called KESTREL was described and applied to the identification of MAPKK and SAPk substrates (22). Since then it has been extended and successfully used to identify substrates of several kinases (23). Here we have adapted this strategy to successfully screen for DAPk substrates. We report the identification of two substrates, ribosomal protein L5 and Mcm3.

L5 proved to be a weak *in vitro* substrate, and its identification in this screen may be due to its high abundance. This contrasts with the S3 substrate, which gave a very strong phosphorylation signal, yet proved refractory to MS analysis due to the low levels of the corresponding protein present (data not shown). Ribosomal proteins are often present as contaminants in MS analysis. However, L5's successful and specific phosphorylation by DAPk suggests that it is the true identity of the S5 substrate. Furthermore, DAPk has previously been shown to phosphorylate a ribosomal protein and influence protein translation rates, at least *in vitro* (18). DAPk's ability to modify ribosomal proteins may be part of a larger signaling checkpoint that monitors ribosomal integrity and translation rates. However, the weak phosphorylation observed precluded further analysis to determine whether L5 is in fact a true *in vivo* substrate of DAPk.

The second substrate discussed here, Mcm3, proved, however, to be a physiologically relevant substrate for DAPk. We showed here that DAPk phosphorylates Mcm3 on Ser160, both *in vitro* and *in vivo*, upon over-expression of the active kinase. Moreover, activation of endogenous DAPk leads to increased Ser160 phosphorylation and the endogenous kinase is necessary for phosphorylation of Mcm3. Mcm3 is one of 6 proteins, Mcm2-7, that form a multi-protein complex which binds and licenses chromatin for initiation of replication (28, 29). Like many of the Mcm proteins, Mcm3 is a known phospho-protein that is phosphorylated in a cell-

cycle dependent manner. These phosphorylation events regulate the cell cycle-dependent recruitment of the Mcm complex to the origin of replication (28, 29). An additional phosphorylation occurs at Ser535 by ATM, in response to ionizing radiation (30). The phosphorylation of Mcm3 on Ser160 is a novel modification with no a priori connection to replication. Ser160 lies within Mcm3's Zinc finger motif, a motif found in all Mcm proteins, although Mcm3's differs from the canonical sequence (28). This motif has been shown to be critical for complex assembly (31). However, mutation of this site to Ala, to mimic dephosphorylation, or to Asp, to mimic constitutive phosphorylation, had no effect on its interaction with other Mcm subunits, or on overall chromatin binding, which requires prior complex assembly (data not shown). Notably, other non-replicative functions of Mcm proteins have been recently described, such as interactions with transcription factors (e.g. 32-34) and gene silencing through the induction of histone deacetylation and heterochromatinization (35). The functional effects of DAPk mediated phosphorylation and any connection to these functions remain to be determined.

In conclusion, the proteomics-based *in vitro* substrate screen employed here has proven an effective strategy for identifying relevant DAPk substrates. It can be broadened to identify the additional substrates that have yet been addressed in this study. Furthermore, it will serve as the basis for further cellular and molecular studies to elucidate the functional significance of the phosphorylation events.

Acknowledgments

We gratefully acknowledge the assistance of Dr. Alla Shainskaya and Tevie Mehlman of the Biological Mass Spectrometry Facility of the Weizmann Institute of Science. We thank Einat

Zalckvar for derivation of pSuper shRNA constructs. This work was supported by a Center of Excellence grant from the Flight Attendant Medical Research Institute (FAMRI) and by a grant from the European Union (LSHB-CT-2004-511983). AK is the incumbent of the Helena Rubinstein Chair of Cancer Research.



References

1. Bialik, S., and Kimchi, A. (2006) The Death-Associated Protein Kinases: structure, function and beyond. *Annu. Rev. Biochem.* 75, 189-210.
2. Deiss, L. P., Feinstein, E., Berissi, H., Cohen, O., and Kimchi, A. (1995) Identification of a novel serine/threonine kinase and a novel 15-kD protein as potential mediators of the gamma interferon-induced cell death. *Genes Dev.* 9, 15-30.
3. Cohen, O., Inbal, B., Kissil, J. L., Raveh, T., Berissi, H., Spivak-Kroizaman, T., Feinstein, E., and Kimchi, A. (1999) DAP-kinase participates in TNF-alpha- and Fas-induced apoptosis and its function requires the death domain. *J. Cell Biol.* 146, 141-148.
4. Jang, C. W., Chen, C. H., Chen, C. C., Chen, J. Y., Su, Y. H., and Chen, R. H. (2002) TGF-beta induces apoptosis through Smad-mediated expression of DAP-kinase. *Nat. Cell Biol.* 4, 51-58.
5. Raveh, T., Droguett, G., Horwitz, M. S., DePinho, R. A., and Kimchi, A. (2001) DAP kinase activates a p19ARF/p53-mediated apoptotic checkpoint to suppress oncogenic transformation. *Nat. Cell Biol.* 3, 1-7.
6. Llambi, F., Lourenco, F. C., Gozuacik, D., Guix, C., Pays, L., Del Rio, G., Kimchi, A., and Mehlen, P. (2005) The dependence receptor UNC5H2 mediates apoptosis through DAP-kinase. *EMBO J.* 24, 1192-1201.
7. Yamamoto, M., Hioki, T., Ishii, T., Nakajima-Iijima, S., and Uchino, S. (2002) DAP kinase activity is critical for C(2)-ceramide-induced apoptosis in PC12 cells. *Eur. J. Biochem.* 269, 139-147.

8. Pelled D, Raveh T, Riebeling C, Fridkin M, Berissi H, Futerman AH, Kimchi A (2002) Death-associated protein (DAP) kinase plays a central role in ceramide-induced apoptosis in cultured hippocampal neurons. *J Biol Chem* 277:1957-1961.
9. Inbal, B., Cohen, O., Polak-Charcon, S., Kopolovic, J., Vadai, E., Eisenbach, L., and Kimchi, A. (1997) DAP kinase links the control of apoptosis to metastasis. *Nature* 390, 180-184.
10. Cohen, O., Feinstein, E., and Kimchi, A. (1997) DAP-kinase is a Ca²⁺/calmodulin-dependent, cytoskeletal-associated protein kinase, with cell death-inducing functions that depend on its catalytic activity. *EMBO J.* 16, 998-1008.
11. Inbal, B., Bialik, S., Sabanay, I., Shani, G., and Kimchi, A. (2002) DAP kinase and DRP-1 mediate membrane blebbing and the formation of autophagic vesicles during programmed cell death. *J. Cell Biol.* 157, 455-468.
12. Wang, W. J., Kuo, J. C., Yao, C. C., and Chen, R. H. (2002) DAP-kinase induces apoptosis by suppressing integrin activity and disrupting matrix survival signals. *J. Cell Biol.* 159, 169-179.
13. Kuo, J. C., Lin, J. R., Staddon, J. M., Hosoya, H., and Chen, R. H. (2003) Uncoordinated regulation of stress fibers and focal adhesions by DAP kinase. *J. Cell Sci.* 116, 4777-4790.
14. Kuo, J., Wang, W., Yao, C., Wu, P., and Chen, R. (2006) The tumor suppressor DAPK inhibits cell motility by blocking the integrin-mediated polarity pathway. *J. Cell Biol.* 172, 619-631.

15. Bialik, S., Bresnick, A. R., and Kimchi, A. (2004) DAP-kinase-mediated morphological changes are localization dependent and involve myosin-II phosphorylation. *Cell Death Differ.* 11, 631-644.
16. Jin, Y., Blue, E. K., Dixon, S., Hou, L., Wysolmerski, R. B., and Gallagher, P. J. (2001) Identification of a new form of death-associated protein kinase that promotes cell survival. *J. Biol. Chem.* 276, 39667-39678.
17. Tian, J. H., Das, S., and Sheng, Z. H. (2003) Ca²⁺-dependent phosphorylation of syntaxin-1A by the death-associated protein (DAP) kinase regulates its interaction with Munc18. *J. Biol. Chem.* 278, 26265-26274.
18. Schumacher, A., Velentza, A., Watterson, D., and Dresios, J. (2006) Death-associated protein kinase phosphorylates Mammalian ribosomal protein s6 and reduces protein synthesis. *Biochemistry* 45, 13614-13621.
19. Shani, G., Marash, L., Gozuacik, D., Bialik, S., Teitelbaum, L., Shohat, G., and Kimchi, A. (2004) Death-associated protein kinase phosphorylates ZIP kinase, forming a unique kinase hierarchy to activate its cell death functions. *Mol. Cell Biol.* 24, 8611-8626.
20. Schumacher, A. M., Schavocky, J. P., Velentza, A. V., Mirzoeva, S., and Watterson, D. M. (2004) A calmodulin-regulated protein kinase linked to neuron survival is a substrate for the calmodulin-regulated death-associated protein kinase. *Biochemistry* 43, 8116-8124.
21. Eisenberg-Lerner, A. and Kimchi, A. (2007) DAP kinase regulates JNK signaling by binding and activating protein kinase D under oxidative stress. *Cell Death Differ.* 14, 1908-15

22. Knebel, A., Morrice, N., and Cohen, P. (2001) A novel method to identify protein kinase substrates: eEF2 kinase is phosphorylated and inhibited by SAPK4/p38delta. *EMBO J.* 20, 4360-4369.
23. Cohen, P., and Knebel, A. (2006) KESTREL: a powerful method for identifying the physiological substrates of protein kinases. *Biochem. J.* 393, 1-6.
24. Shohat, G., Spivak-Kroizman, T., Cohen, O., Bialik, S., Shani, G., Berrisi, H., Eisenstein, M., and Kimchi, A. (2001) The pro-apoptotic function of death-associated protein kinase is controlled by a unique inhibitory autophosphorylation-based mechanism. *J. Biol. Chem.* 276, 47460-47467.
25. Schories, B., Engel, K., Dorken, B., Gossen, M., and Bommert, K. (2004) Characterization of apoptosis-induced Mcm3 and Cdc6 cleavage reveals a proapoptotic effect for one Mcm3 fragment. *Cell Death Differ.* 11, 940-942.
26. Schwab, B., Leist, M., Knippers, R., and Nicotera, P. (1998) Selective proteolysis of the nuclear replication factor MCM3 in apoptosis. *Exp. Cell Res.* 238, 415-421.
27. Velentza, A.V., Schumacher, A.M., Weiss, C., Egli, M., and Watterson, D.M. (2001) A protein kinase associated with apoptosis and tumor suppression: structure, activity, and discovery of peptide substrates. *J. Biol. Chem.* 276, 38956-38965
28. Forsburg, S. (2004) Eukaryotic MCM proteins: beyond replication initiation. *Microbiol. Mol. Biol. Rev.* 68, 109-131.
29. Tye, B. (1999) MCM proteins in DNA replication. *Annu. Rev. Biochem.* 68, 649-686.

30. Cortez, D., Glick, G., and Elledge, S. (2004) Minichromosome maintenance proteins are direct targets of the ATM and ATR checkpoint kinases. *Proc. Natl. Acad. Sci. USA* 101, 10078-10083.
31. Fletcher, R., Bishop, B., Leon, R., Sclafani, R., Ogata, C., and Chen, X. (2003) The structure and function of MCM from archaeal *M. Thermoautotrophicum*. *Nat. Struct. Biol.* 10, 160-167.
- 3435.
32. Zhang, J., Zhao, Y., Chait, B., Lathem, W., Ritzi, M., Knippers, R., and Darnell, J., Jr. (1998) Ser727-dependent recruitment of MCM5 by Stat1alpha in IFN-gamma-induced transcriptional activation. *EMBO J.* 17, 6963-6971.
33. DaFonseca, C., Shu, F., and Zhang, J. (2001) Identification of two residues in MCM5 critical for the assembly of MCM complexes and Stat1-mediated transcription activation in response to IFN-gamma. *Proc. Natl. Acad. Sci. USA* 98, 3034-3039.
34. Snyder, M., He, W., and Zhang, J. J. (2005) The DNA replication factor MCM5 is essential for Stat1-mediated transcriptional activation. *Proc. Natl. Acad. Sci. USA* 102, 14539-14544.
35. Gonzalez, S., Klatt, P., Delgado, S., Conde, E., Lopez-Rios, F., Sanchez-Céspedes, M., Mendez, J., Antequera, F., and Serrano, M. (2006) Oncogenic activity of Cdc6 through repression of the INK4/ARF locus. *Nature* 440, 702-706.

Figure Legends

Figure 1. Assay for *in vitro* DAPk substrates. Total HeLa cell lysate was incubated in kinase assays with or without DK1 (1 μ g), and reactions were resolved by 10% SDS-PAGE. Specific phosphorylated substrates appearing only in the presence of DK1 are indicated and labeled S1-S9. Autophosphorylation of DK1, which is enhanced in the absence of competing substrate, is indicated.

Figure 2. Purification of DAPk substrates. **A.** The 60% salt precipitate (input) was fractionated by hydrophobic column chromatography with decreasing concentrations of NH_4SO_4 and selected fractions were analyzed for the presence of S5 substrate in kinase assays. Reactions were resolved on a 10% gel which was stained with silver (left), dried and exposed to film (right). FT, flow-through and washes. As a control for specificity, fraction #29 was incubated in the absence of DK1 (-). **B.** The 50% salt precipitate was fractionated and alternate fractions were analyzed for the presence of S9 substrate in kinase assays as described above. Fractions below #16 represent flow-through and washes. As a control for specificity, fraction #30 was incubated in the absence of DK1 (-).

Figure 3. Identification of S5 as ribosomal protein L5. **A.** Flag-tagged L5 was expressed in and immunopurified from 293T cells and 400 ng of the purified protein was subjected to kinase assays in the presence or absence of DK1. Equimolar concentrations of recombinant His-tagged MLC or Flag-tagged GFP were used as positive and negative controls, respectively. Reactions were resolved on 10% gels which were stained with gelcode (bottom), dried and exposed to film to visualize substrates (top). **B.** Flag-tagged L5 (400 ng) was incubated with full length Flag-

tagged DAPk (at a kinase:substrate ratio of 1:10) in the presence of Ca^{2+} /CaM or EGTA with limiting concentrations of hot ATP and assayed as above. *, unidentified phosphorylated bands that co-immunoprecipitate with L5; IgG HC and LC, contaminating heavy and light chains of antibody used to purify Flag-DAPk.

Figure 4. Identification of S9 as Mcm3. A-C. Flag-tagged Mcm3 was expressed in and immunopurified from 293T cells and 1 μg of the purified protein was subjected to kinase assays in the presence or absence of DK1 (at a kinase:substrate ratio of 1:5) (**A**) or full length Flag-tagged DAPk WT (at a kinase:substrate ratio of 1:10) (**B**) or mutant K42A (**C**) in the presence of Ca^{2+} /CaM or EGTA. Equimolar concentrations of recombinant His-tagged MLC or Flag-tagged α -actinin4 were used as positive and negative controls, respectively. Reactions were resolved on 7.5% gels which were stained with gelcode (**B,C** bottom), dried and exposed to film to visualize substrates (**A** and **B,C** top). **D.** Flag-Mcm3 (800 ng) was incubated with full length DAPk at a kinase:substrate ratio of 1:10 from 1 min to 2 h. Reactions were resolved on a 7.5% gel and the extent of incorporation of radiolabeled ATP was quantitated by PhosphoImaging to determine the stoichiometry of phosphorylation. Data is reported as mol total ATP incorporated/mol Mcm3.

Figure 5. Mcm3 is phosphorylated by DAPk on Ser 160. A. Alignment of Mcm3 aa 152-163 with the DAPk phosphorylation site of several known substrates and a synthetically derived peptide substrate with an optimal k_m , as reported by (39). The proposed consensus phosphorylation site of DAPk is indicated above the sequences. **B.** Mcm3 WT or S160A mutant was subjected to kinase assays with full length Ca^{2+} /CaM-activated DAPk. Reactions were

resolved on a 7.5% gel which was stained with gelcode (bottom), dried and exposed to film (top). **C.** Quantitation of extent of phosphorylation of increasing concentrations of either Mcm3 WT or S160A mutant by full length DAPk. Reactions were resolved on a 7.5% gel and the extent of incorporation of radiolabeled ATP was quantitated by PhosphoImaging. **D.** Kinase assays were performed with full length DAPk in the absence of radio-labeled ATP, with increasing concentrations of either WT or S160A Mcm3. Reactions were resolved by SDS-PAGE and Western blotted with a phospho-Ser160 specific antibody. A reproduction of the Ponceau S-stained membrane is shown to estimate protein levels.

Figure 6. Kinetic analysis of Mcm3 phosphorylation. Kinase assays were performed using increasing concentrations of the Mcm3 peptide shown in Fig. 5A with DK1. Reactions were blotted onto P-81 filters, and phosphorylation levels were quantitated by scintillation counting. Data is reported as the total ATP (pmol) incorporated per μ g of DK1 (**A**) and the double reciprocal blot (1/V vs. 1/S, **B**).

Figure 7. DAPk phosphorylates Mcm3 *in vivo*. **A.** Lysates from 293T cells transfected with DAPk \square CaM, K42A or as a control, Luc, were immunoprecipitated with antibodies to Mcm3 and blotted with antibodies to phosphoSer160 or to total Mcm3 to determine levels of Mcm3 captured. Left panel: Western blot of total cell lysate indicating levels of transfected DAPk and endogenous Mcm3. **B.** Lysates from 293T cells treated with 10 μ M ionomycin or DMSO for 30 min were immunoprecipitated with antibodies to Mcm3 and blotted with antibodies to Mcm3 phosphoSer160 or to total Mcm3 to determine levels of Mcm3 captured. **C.** 293T cells were transfected with shRNA targeting DAPk or HC-Red and 5 days later, were treated with DMSO

or ionomycin as above. Left panel, blot of total cell lysate indicating knock-down of DAPk, and as a loading control, the closely related ZIPk. Right panel, lysates were immunoprecipitated with antibodies to Mcm3 and blotted with either antibodies to Mcm3 phosphoSer160 or total Mcm3.

Table I: Results of MS/MS analysis of S5.

The band corresponding to substrate S5 in phenyl-HP hydrophobic column fraction 20 (fractionation of the 60% NH₄SO₄ precipitant) was excised from an SDS acrylamide gel and subjected to MS/MS analysis. Annexin II was eliminated as a candidate after it failed to undergo phosphorylation in *in vitro* kinase assays with either DK1 or full length DAPk (data not shown).

candidate	Accession # (Swiss-Prot)	MW (kDa)	Score	# Peptides	Sequence Coverage
Ribosomal protein L5	P46777	28	285	3	16%
Annexin II	P07355	38	268	8	32%
Na ⁺ /K ⁺ ATPase 1 α 1	P05023	114	97	3	3%
Protein phosphatase PP1 α	P62140	37	64	3	11%
Caspase-7	P55210	34	37	2	5%
Aldose reductase	P15121	36	35	3	13%

Table II: Results of MS/MS analysis of S9.

The bands corresponding to substrate S9 in phenyl-HP hydrophobic column fractions 36 and 41 (fractionation of the 50% NH₄SO₄ precipitant) were excised from SDS acrylamide gels and subjected to MS/MS analysis. The use of two fractions from either end of the elution range enabled elimination of contaminating proteins that were present in one, but not both, fractions, and only those common to both are listed. α -actinin-4 was eliminated as a candidate after it failed to undergo phosphorylation in *in vitro* kinase assays with either DK1 or full length DAPk (data not shown).

Candidate	Accession # (Swiss-Prot)	MW (kDa)	Fraction 36			Fraction 41		
			Score	# Peptides	Sequence Coverage	Score	# Peptides	Sequence Coverage
Mcm3	P25205	91	274	16	33%	108	10	20%
α -actinin-4	O43707	105	231	21	32%	42	9	14%
Mcm6	Q14566	93	109	9	14%	129	12	33%
Glucosidase-II α	Q14697	107	102	7	12%	55	4	7%
HSPA4L (OSP94)	O95757	95	98	9	17%	130	7	11%
UBP5	P45974	96	72	8	15%	40	7	15%
C1-tetrahydrofolate synthase	P11586	102	57	5	8%	112	8	12%
4F2hc	P08195	58	40	2	4%	32	4	10%
NSUN2	Q08J23	86	30	2	-	48	5	7%

Figure 1

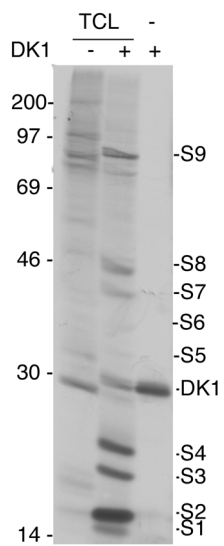


Figure 3

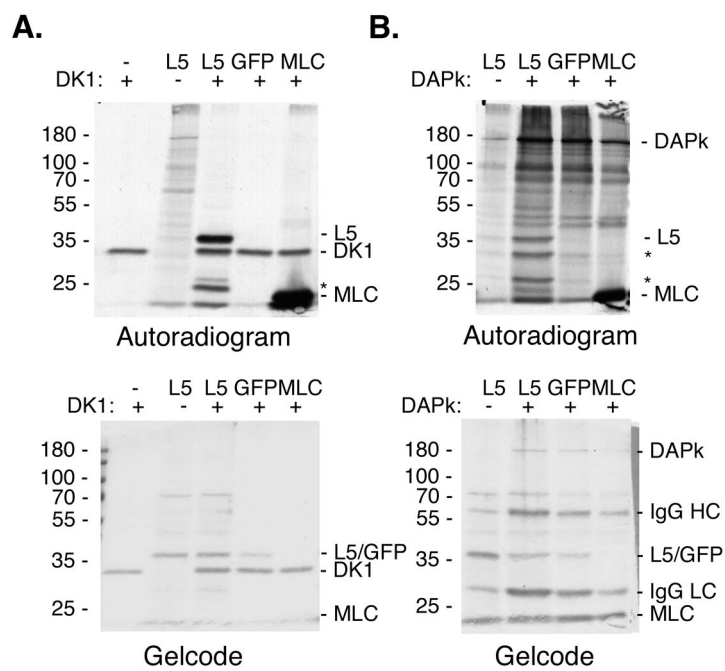


Figure 4

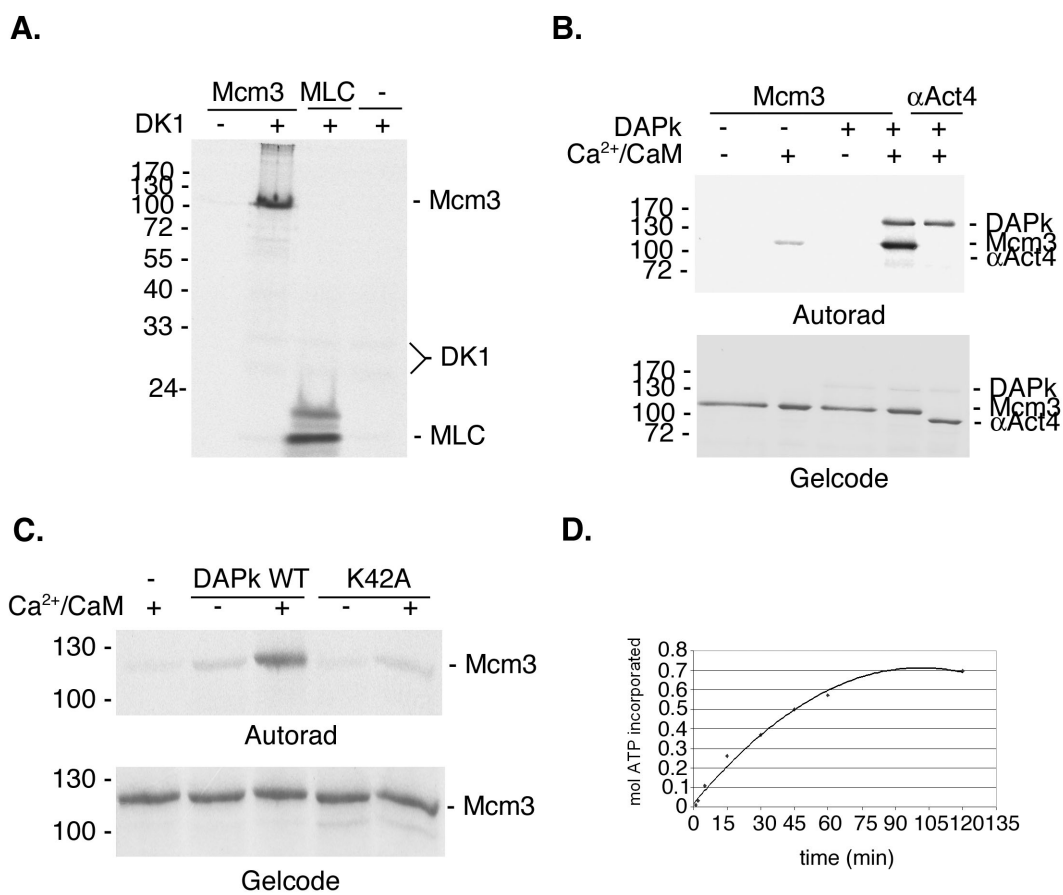


Figure 5

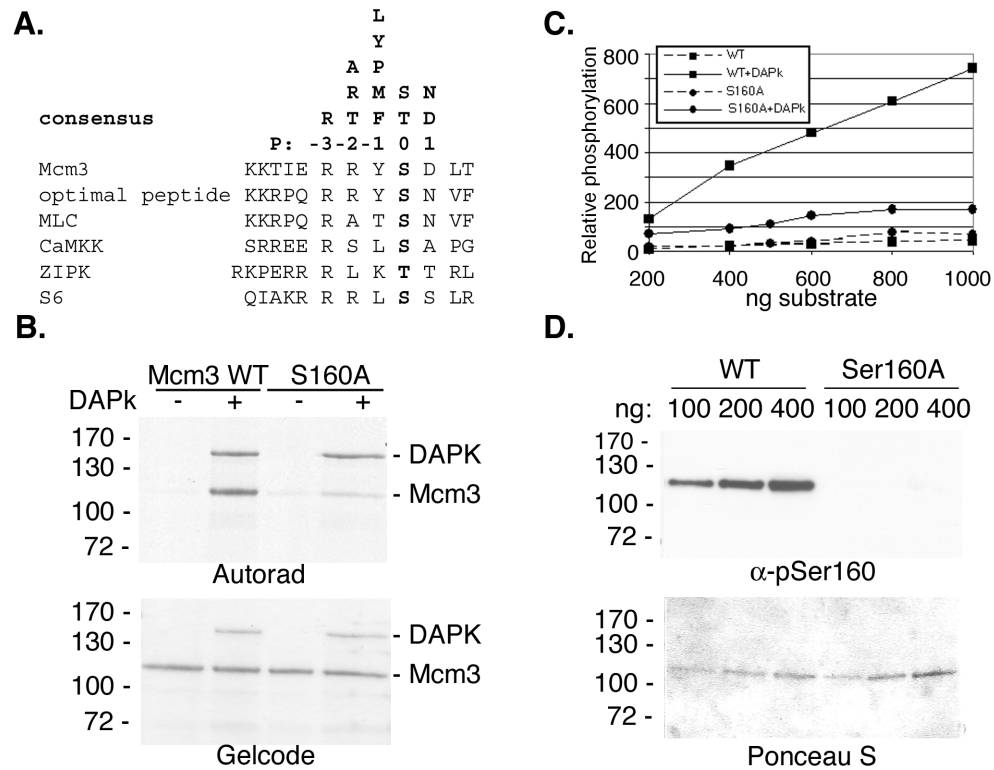
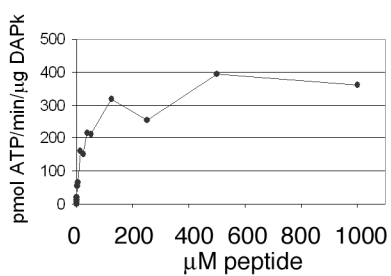


Figure 6

A.



B.

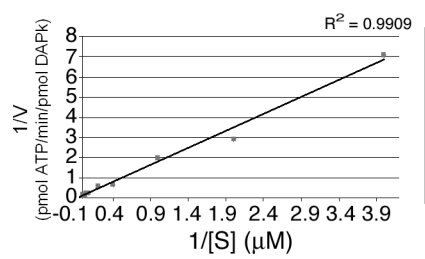


Figure 7

